SCIENCE CHINA
Life Sciences

•LETTER TO THE EDITOR•

June 2022 Vol.65 No.6: 1259–1262
https://doi.org/10.1007/s11427-021-2049-6

Genetically encoded redox biosensor system for H_2O_2 measurement in four subcellular compartments in acute myeloid leukemia (AML) cells

Mengmeng Cui[1], Ghulam Abbas[1,3], Dianbing Wang[1], Qian Liu[1], Rui Gong[1,3], Min Li[1] & Xian-En Zhang[1,2,3*]

[1]*National Laboratory of Biomacromolecules, Institute of Biophysics, Chinese Academy of Sciences, Beijing 100101, China;*
[2]*Faculty of Synthetic Biology, Shenzhen Institute of Advanced Technology, Chinese Academy of Sciences, Shenzhen 518055, China;*
[3]*University of Chinese Academy of Sciences, Beijing 100049, China*

Received October 7, 2021; accepted December 20, 2021; published online February 17, 2022

Citation: Cui, M., Abbas, G., Wang, D., Liu, Q., Gong, R., Li, M., and Zhang, X.E. (2022). Genetically encoded redox biosensor system for H_2O_2 measurement in four subcellular compartments in acute myeloid leukemia (AML) cells. Sci China Life Sci 65, 1259–1262. https://doi.org/10.1007/s11427-021-2049-6

Dear Editor,

Acute myeloid leukemia (AML) is an aggressive form of a hematological neoplastic disorder induced by the oncogenic transformation of hematopoietic stem and myeloid progenitor cells (Bossis et al., 2014). In the treatment of AML, the major mechanism of chemotherapeutic therapy is widely acknowledged as the induction of excessive reactive oxygen species (ROS) and ROS levels are relatively up-regulated in AML and many other cancers (Irwin et al., 2013). Therefore, ROS are considered as the vital constituent for effective AML therapy. The spatiotemporal distribution of ROS in cells is not uniform but highly dynamic and compartmentalized (Zou et al., 2018). H_2O_2, the representative ROS, acts as a secondary messenger in various redox signaling cascades depending on their subcellular distribution and communication (Irwin et al., 2013).

In vivo ROS measurement is based on ROS-specific fluorescent probes (Belousov et al., 2006; Provost et al., 2010), either chemical fluorescent probes or genetically-encoded fluorescent probes. Exogenous chemical probes are characterized with high specificity and sensitivity. However, being exogenous to cells may have an unpredictable effect on cell growth and metabolism (Passos et al., 2013). Endogenous genetically encoded fluorescent sensors can achieve the real-time and dynamic detection of ROS in living cells or different subcellular compartments without toxic effect, such as HyPer family (Belousov et al., 2006), which is based on the fusion of the H_2O_2-sensing domain of *E. coli* oxyR, with a circularly permutated yellow fluorescent protein (cpYFP), allowing a ratiometric measurement of H_2O_2 levels with high sensitivity and reversibility. Likewise, TriPer is developed by replacement of OxyR alanine 187 in HyPer with cysteine, which is suitable for H_2O_2 detection in a relatively oxidized environment like endoplasmic reticulum (ER) (Melo et al., 2017).

Although, there has been extensive research on basic and clinical aspects of the AML, the introduction of exogenous genes in AML cells is difficult, the AML cells remain to be a sort of "hard-to-transfect" cells (Basiouni et al., 2012). So far, ROS biosensors for AML research is barely explored. In this study, we used HyPer and TriPer as sensing modules and subcellular localization guide peptides, and adopted lentivirus transfection and repeated high-throughput fluorescence-activated cell sorting (FACS). Finally, we successfully constructed a sensor system for measurement of H_2O_2 level in four subcellular compartments: cytosol, nucleus, mitochondria, and ER of AML cells (Cyto-HyPer, NLS-HyPer,

*Corresponding author (email: zhangxe@ibp.ac.cn)

MLS-HyPer, and ER-TriPer), which was confirmed by high-resolution imaging with SIM (Figure 1A1–A12). To characterize the sensitivity and dynamic response of HyPer and TriPer in AML cells, we performed the ratiometric calibration in the Cyto-HyPer, NLS-HyPer, MLS-HyPer, and ER-TriPer stable cell lines, which was determined with H_2O_2 stimulus by flow cytometry, respectively. Cyto-HyPer, NLS-HyPer, and MLS-HyPer showed a strong response to exogenous H_2O_2 stimulus with concentration range up to 100 μmol L^{-1} and detection limit of 5 μmol L^{-1} (Figure 1C). While, TriPer showed a strong response to H_2O_2 with concentration range up to 150 μmol L^{-1} with a detection limit of 5 μmol L^{-1} (Figure 1D). The response of Cyto-HyPer and NLS-HyPer reached their maximum with 100 μmol L^{-1} H_2O_2 after 2 min (Figure 1E). While, the response of MLS-HyPer and ER-TriPer reached their peak with 100 μmol L^{-1} H_2O_2 after 20 min (Figure 1E and F). Furthermore, the pH-sensitive SypHer sensor was stably expressed in AML cells to ensure the fluctuations in fluorescence signals are not due to pH variations, while the pH almost remained unchanged after H_2O_2 treatment (Figure S1A and B in Supporting Information). These results depict HyPer and TriPer can be applied for the real-time and dynamic detection of H_2O_2 level in AML cells.

The H_2O_2 basal level in mitochondria was found to be the highest followed by the cytosol and the lowest in the nucleus based on the response of HyPer, while ER exhibited a high H_2O_2 basal level according to the response of TriPer (Figure 1B). However, the basal level of H_2O_2 in the nucleus showed higher than cytoplasm of human endocardial cells, detected by the chemical probe H_2DCFDA (Provost et al., 2010). It is not yet clear whether the difference in results is due to the respective properties of different cells or exogenous chemical probes themselves might have subtle interference to the intracellular environment that is unlikely to occur by the genetically encoded endogenous sensors. While the endogenous biosensors may truly reflect the basic levels of H_2O_2 in the various subcellular compartments in leukemia cells. Moreover, considering the ROS level vary among different cancer types and there is also intercellular H_2O_2 communication among distinct subcellular compartments, it makes sense to compare ROS levels in AML cells with hematopoietic stem cells and other cancer cells, and monitor the inter-compartmental communication dynamically using the endogenous biosensor system.

The effect of drug treatment of AML was systematically investigated by using this sensor system. At the whole-cell level, cisplatin-induced the production of H_2O_2 in AML cells to cause the cell death (Figures S1C and S2A in Supporting Information); resveratrol demonstrated the bidirectional regulation of H_2O_2 in AML cells (Figure S1D in Supporting Information), Prussian blue nanoparticles (PBNPs) can reduce the H_2O_2 level (Figure S1E in Supporting Information), while Fe_3O_4 nanoparticles (NPs) promote the H_2O_2 generation (Figure S1G in Supporting Information). The results showed that there is a common mechanism i.e., the alteration of ROS level caused by drugs is highly associated with cell death in various cancers including AML. Based on the discovery of the effect of individual drugs on cellular ROS and cell death (Figures S1E, S1G, S2C, and S2E in Supporting Information), we further explored the effect of combined drug therapy. Interestingly, PBNPs and Fe_3O_4 NPs combined with Ara-C (cytarabine) keep the potency to regulate the H_2O_2 level in AML cells (Figure S1F and H in Supporting Information). The combined therapy of PBNPs and Ara-C may reduce the killing effect on tumor cells (Figure S2D in Supporting Information), while the combination of Fe_3O_4 NPs and Ara-C can promote cell death or enhance the efficacy of Ara-C (Figure S2F in Supporting Information). These findings imply that the sensor system may help to optimize the drug treatment scheme to improve the therapeutical effect of AML.

The distribution of ROS is compartmentalized in cells, and the response of subcellular ROS level to anticancer drugs is complex in AML cells, which needs in-depth research. Using the sensor system, we have determined the effect of various typical chemotherapeutic drugs (Ara-C, paclitaxel, and doxorubicin) on different subcellular H_2O_2 level in AML cells. We observed that all three drugs could increase the H_2O_2 level in all four subcellular compartments and induce cell death (Figure 1G–L; Figure S2G–I in Supporting Information). The response ratio of MLS-HyPer was maximum upon treatment with 2.5 μg mL^{-1} doxorubicin, and about 4-fold signal change was recorded, implying mitochondrial H_2O_2 level was the most sensitive to doxorubicin as compared to the cytosol, nucleus, and ER (Figure 1G and H). Therefore, mitochondria could be a major target of doxorubicin in the treatment of AML. These results can help for further exploring the role of ROS-related pathways and developing the system for mitochondrial-targeted doxorubicin delivery. Interestingly, as compared to the other compartments, the response ratio of MLS-HyPer reached the plateau at the lowest concentration of Ara-C (1 μmol L^{-1}) and paclitaxel (2.5 μmol L^{-1}), and NES-HyPer displayed the most change of normalized ratio around 4-fold (Figure 1I–L). Thus, AML cells with higher ROS levels of cytosol and mitochondria were more sensitive to Ara-C and paclitaxel. The drug resistance of Ara-C and paclitaxel in cancer treatments, such as leukemia and ovarian cancer, might be linked to ROS (Agarwal and Kaye, 2003; Bosc et al., 2017). Both drugs targeting mitochondrial oxidative metabolism and the knockdown of nuclear factor erythroid 2-related factor 2, one major cellular antioxidant system, can sensitize the resistant cell to Ara-C in AML (Bosc et al., 2017). And paclitaxel-resistant cells were found to contain alterations in ROS-induced oxidative stress-related genes' expression, such as

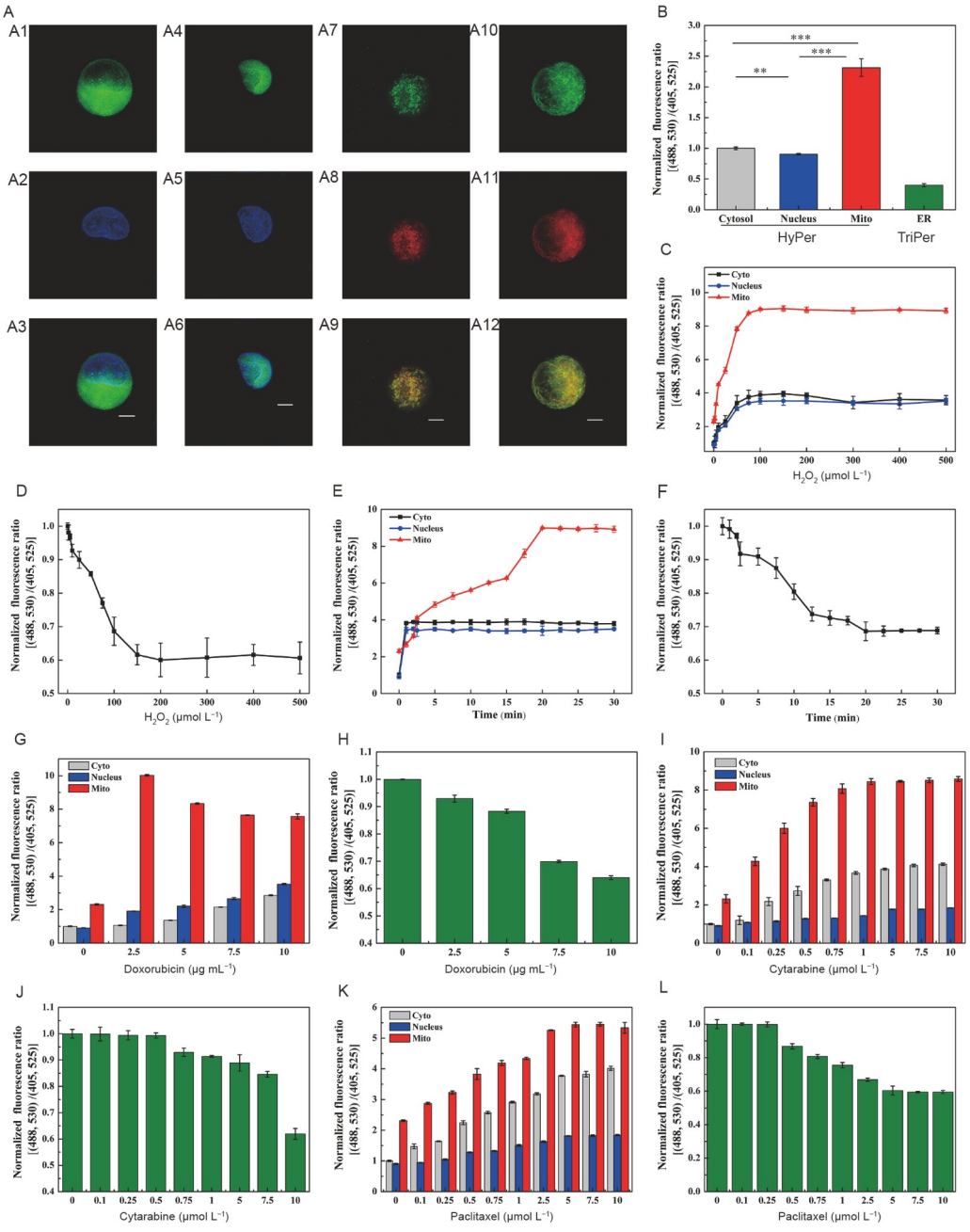

Figure 1 Intracellular localization of HyPer and TriPer targeted to various subcellular compartments in HL60 cells and their response to H_2O_2, and different chemotherapeutic drugs. A, Panels represent the live-cell imaging of HyPer stably expressed in the cytosol (A1, A2, and A3), nucleus (A4, A5, and A6), and mitochondria (A7, A8, and A9) while TriPer stably expressed in the ER (A10, A11, and A12) of HL60 cells by SIM. Panels A2 and A5 show staining with Hoechst 33342, A8 with Mito-Tracker Red, and A11 with ER-Tracker Red. Panels A3 and A6 are merged with Hoechst 33342 staining, A9 with Mito-Tracker Red, and A12 with ER-Tracker Red. Scale bar: 5 μm. B, The normalized fluorescence ratio of HyPer and TriPer excited by 488 and 405 nm lasers of flow cytometry (≥10,000 cells). C, The normalized response ratio (488/405 nm) of HyPer stably expressed in the cytosol, nucleus and mitochondria of HL60 cells after H_2O_2 (0–500 μmol L^{-1}) treatment by flow cytometry (≥10,000 cells). Treatment time: 2 min for cytosol and nucleus, 20 min for mitochondria. D, The normalized ratio (488/405 nm) of TriPer stably expressed in the ER of HL60 cells 20 min after H_2O_2 (0–500 μmol L^{-1}) treatment by flow cytometry (≥10,000 cells). E, The normalized response ratio (488/405 nm) of HyPer stably expressed in the cytosol, nucleus and mitochondria of HL60 cells after H_2O_2 treatment (100 μmol L^{-1},0–30 min) by flow cytometry (≥10,000 cells). F, The normalized ratio (488/405 nm) of TriPer stably expressed in the ER of HL60 cells after H_2O_2 (100 μmol L^{-1},0–30 min) treatment by flow cytometry (≥10,000 cells). G–L, The normalized response ratio (488/405 nm) of Cyto-HyPer, NLS-HyPer, MLS-HyPer, and ER-TriPer to doxorubicin (G, H), cytarabine (I, J) and paclitaxel (K, L) by flow cytometry (≥10,000 cells). Drug treatment time: 24 h. The data was acquired with FACSAria IIIu (BD Biosciences, USA) flow cytometry using 488 and 405 nm as excitation wavelengths as well as 530/30 nm and 525/50 nm filter sets for emission. Data are presented as mean±SD, n≥3. One-way analysis of variance (ANOVA) was used to compare the differences between different groups (***, P<0.001; **, P<0.01; *, P<0.05). All the doxorubicin-treated groups are significantly different from the control group. While, all the cytarabine-treated groups are significantly different from the control group except the 0.1, 0.25, and 0.5 μmol L^{-1} cytarabine-treated groups of ER-TriPer, and Except the 0.1 and 0.25 μmol L^{-1} paclitaxel-treated groups of ER-TriPer, all the paclitaxel -treated groups are significantly different from the control group.

UGT1A6, MAOA, and CYBA (Agarwal and Kaye, 2003). So, the monitoring and precisely regulating the cytosolic and mitochondrial ROS level, and exploring their link to the corresponding genes' activity in AML cells might offer an avenue to improve the therapeutic effects.

In summary, we have successfully constructed the genetically encoded fluorescent H_2O_2 sensor-system for measurement of ROS level in four subcellular compartments in AML suspension cells. The newly established AML H_2O_2 sensor-system allows us to profile ROS basal level at the subcellular level and investigate the drug-sensitive compartments in AML cells. We found that the basic H_2O_2 levels of the four compartments in AML cells are very distinguishable and that each compartment responds differently to drug treatments, with mitochondria and cytoplasm the most sensitive to anti-AML drugs. The findings demonstrate the endogenous biosensor-system will become a promising tool to deeply understand the cytopathy occurrence and drug mechanism in AML, and develop more effective AML treatment strategies.

Compliance and ethics *The author(s) declare that they have no conflict of interest.*

Acknowledgements *This work was supported by the National Key Research and Development Program of China (2017YFA0205500 and 2018YFA0902702), the National Natural Science Foundation of China (21890743), and the Strategic Priority Research Program of the Chinese Academy of Sciences (XDB29050100). We thank Junying Jia and Shu Meng for technical assistance in FACS analysis (FACS center, Institute of Biophysics (IBP), Chinese Academy of Sciences (CAS)) and Shuoguo Li and Yan Teng (Center for Biological Imaging (CBI), IBP-CAS) for SIM imaging. We gratefully acknowledge Prof. Yu Zhang for Nanoparticles support (Southeast University, Nanjing, China).*

References

Agarwal, R., and Kaye, S.B. (2003). Ovarian cancer: strategies for overcoming resistance to chemotherapy. Nat Rev Cancer 3, 502–516.

Basiouni, S., Fuhrmann, H., and Schumann, J. (2012). High-efficiency transfection of suspension cell lines. Biotechniques 53, 1–4.

Belousov, V.V., Fradkov, A.F., Lukyanov, K.A., Staroverov, D.B., Shakhbazov, K.S., Terskikh, A.V., and Lukyanov, S. (2006). Genetically encoded fluorescent indicator for intracellular hydrogen peroxide. Nat Methods 3, 281–286.

Bosc, C., Selak, M.A., and Sarry, J.E. (2017). Resistance is futile: targeting mitochondrial energetics and metabolism to overcome drug resistance in cancer treatment. Cell Metab 26, 705–707.

Bossis, G., Sarry, J.E., Kifagi, C., Ristic, M., Saland, E., Vergez, F., Salem, T., Boutzen, H., Baik, H., Brockly, F., et al. (2014). The ROS/SUMO axis contributes to the response of acute myeloid leukemia cells to chemotherapeutic drugs. Cell Rep 7, 1815–1823.

Irwin, M.E., Rivera-Del Valle, N., and Chandra, J. (2013). Redox control of leukemia: from molecular mechanisms to therapeutic opportunities. Antioxid Redox Signal 18, 1349–1383.

Melo, E.P., Lopes, C., Gollwitzer, P., Lortz, S., Lenzen, S., Mehmeti, I., Kaminski, C.F., Ron, D., and Avezov, E. (2017). TriPer, an optical probe tuned to the endoplasmic reticulum tracks changes in luminal H_2O_2. BMC Biol 15, 24.

Passos, J.F., Miwa, S., and von Zglinicki, T. (2013). Measuring reactive oxygen species in senescent cells. In: Galluzzi, L., Vitale, I., Kepp, O., and Kroemer, G., eds. Cell Senescence. Methods in Molecular Biology (Methods and Protocols). Totowa: Humana Press. 253–263.

Provost, C., Choufani, F., Avedanian, L., Bkaily, G., Gobeil, F., and Jacques, D. (2010). Nitric oxide and reactive oxygen species in the nucleus revisited. Can J Physiol Pharmacol 88, 296–304.

Zou, Y., Wang, A., Shi, M., Chen, X., Liu, R., Li, T., Zhang, C., Zhang, Z., Zhu, L., Ju, Z., et al. (2018). Analysis of redox landscapes and dynamics in living cells and *in vivo* using genetically encoded fluorescent sensors. Nat Protoc 13, 2362–2386.

SUPPORTING INFORMATION

The supporting information is available online at https://doi.org/10.1007/s11427-021-2049-6. The supporting materials are published as submitted, without typesetting or editing. The responsibility for scientific accuracy and content remains entirely with the authors.